J. Membrane Biol. 173, 187–201 (2000)

The Journal of
Membrane
Biology

Influence of a Transmembrane Protein on the Permeability of Small Molecules Across Lipid Membranes

T.-X. Xiang, B.D. Anderson
Department of Pharmaceutics & Pharmaceutical Chemistry, University of Utah, Salt Lake City, UT 84112, USA

Received: 12 July 1999/Revised: 20 October 1999

Abstract. The influence of the nonchannel conformation of the transmembrane protein gramicidin A on the permeability coefficients of neutral and ionized α-X-*p*-methyl-hippuric acid analogues (XMHA) (X = H, OCH_3, CN, OH, COOH, and $CONH_2$) across egg-lecithin membranes has been investigated in vesicle efflux experiments. Although 10 mol% gramicidin A increases lipid chain ordering, it enhances the transport of neutral XMHA analogues up to 8-fold, with more hydrophilic permeants exhibiting the greatest increase. Substituent contributions to the free energies of transfer of both neutral and anionic XMHA analogues from water into the bilayer barrier domain were calculated. Linear free-energy relationships were established between these values and those for solute partitioning from water into decadiene, chlorobutane, butyl ether, and octanol to assess barrier hydrophobicity. The barrier domain is similar for both neutral and ionized permeants and substantially more hydrophobic than octanol, thus establishing its location as being beyond the hydrated headgroup region and eliminating transient water pores as the transport pathway for these permeants, as the hydrated interface or water pores would be expected to be more hydrophilic than octanol. The addition of 10 mol% gramicidin A alters the barrier domain from a decadiene-like solvent to one possessing a greater hydrogen-bond accepting capacity. The permeability coefficients for ionized XMHAs increase with Na^+ or K^+ concentration, exhibiting saturability at high ion concentrations. This behavior can be quantitatively rationalized by Gouy-Chapman theory, though ion-pairing cannot be conclusively ruled out. The finding that transmembrane proteins alter barrier selectivity, favoring polar permeant transport, constitutes an important step toward understanding permeability in biomembranes.

Key words: Permeability — Gramicidin A — Partition coefficients — Lipid bilayers — Membrane transport — Linear free-energy relationships

Introduction

Biomembranes, commonly described as a fluid mosaic of proteins embedded within a lipid bilayer matrix (Singer & Nicolson, 1972), function as a barrier to transport of chemical species involved in various life processes and as a matrix on which various biochemical reactions may occur. Although the transport of many molecular species (e.g., glucose, amino acids, metal ions, etc.) of biological interest involves carriers and channel proteins, passive diffusion within biomembranes is the predominant mechanism for many permeants, including lipophilic drug molecules as well as low molecular weight polar compounds. Because of this fundamental importance, extensive investigations of the passive permeation of small molecules have been undertaken in the past several decades using various model membranes, especially protein-free lipid bilayers (Haydon & Hladky, 1972; Finkelstein, 1976; Carruthers & Melchior, 1983; Walter & Gutknecht, 1986; Xiang, Chen & Anderson, 1992; Clerc & Thompson, 1995; Lande, Donovan & Zeidel, 1995; Xiang & Anderson, 1997; Paula, Volkov & Deamer, 1998). These studies have provided insight into the mechanisms by which the chemical composition of bilayer lipids (e.g., the acyl chain length, degree of unsaturation, and headgroup charges) and the physical states of the membranes (e.g., phase structure, surface pressure, and temperature) affect permeation.

Nevertheless, one of the principal and as yet unre-

Correspondence to: B.D. Anderson

solved issues in understanding molecular permeation mechanisms in biomembranes is the role membrane proteins play in determining passive permeation rates across biomembranes. While intensive efforts have been devoted to understanding the mechanisms for various protein-assisted transport processes (e.g., carriers, channels, and pumps), it is somewhat surprising that so little is known about the mechanisms by which these proteins alter basal permeability properties of biomembranes. Among the important questions that need to be addressed are: (i) How strongly do membrane proteins affect basal permeabilities of neutral and ionic small molecule permeants? (ii) Can the effects of membrane proteins be explained in terms of structural changes (e.g., ordering and hydrophobicity) of the lipid chains within the membranes due to the presence of these membrane proteins (Muller, van Ginkel & van Faassen, 1996; Subczynski et al., 1998)? (iii) Do membrane proteins alter the pathway(s) through which permeants diffuse across membranes? and (iv) How do these effects depend on the nature, conformation, and amount of membrane proteins and their location in the membranes (i.e., peripheral *vs.* integral)?

Biomembranes varying in lipid and protein composition differ markedly in their chemical selectivity to solute transport. For example, studies in the authors' laboratories have shown that the barrier domain for transport across human stratum corneum, the barrier properties of which are generally attributed to the multiple lamellae of lipid bilayers localized within its intercellular spaces, closely resembles octanol in its selectivity to permeant structure (Anderson, Higuchi & Raykar, 1988; Anderson & Raykar, 1989). Similar correlations between solute transport across the blood-brain barrier and partition coefficients in octanol are well established (Rapoport, Ohno & Pettigrew, 1979; Levin, 1980). In contrast, the barrier domain within protein-free liquid-crystalline lipid membranes resembles that of a nonpolar solvent (e.g., decadiene) with negligible hydrogen bonding capacity (Walter & Gutknecht, 1986; Xiang et al., 1992; Xiang & Anderson, 1994b).

It is very difficult to explore the above fundamental issues in natural biomembranes where the distribution and structure of various membrane proteins are unknown. Therefore, we attempt in this paper to shed light on the first three questions by investigating the effects on solute basal permeability of a model transmembrane protein, gramicidin A (gA), reconstituted into phospholipid bilayers in its nonchannel conformation. Gramicidin A is a member of a large family of polypeptide antibiotics produced by *Bacillus brevis*, an aerobic soil bacterium. It consists of 15 amino acid residues, the sequence of which from its N- to C-terminus is formyl-Val_1-Gly_2-Ala_3-Leu_4-Ala_5-Val_6-Val_7-Val_8-Trp_9-Leu_{10}-Trp_{11}-Leu_{12}-Trp_{13}-Leu_{14}-Trp_{15}-ethanolamine with alternating L and D chirality (Anderson, 1984; Cornell, 1987). Gramicidin A is almost insoluble in water and can easily span certain bilayers in either a channel conformation where gA forms right-handed head-to-head single helical dimers with two monomers joined at their N-termini at the bilayer center or a nonchannel conformation where gA forms double-helical head-to-tail dimers depending on the organic solvent history for its incorporation into the membranes (Wallace, 1990; Killian, 1992). As a membrane-spanning, relatively simple, hydrophobic polypeptide, gramicidin has become a prototype for studies of protein-lipid model systems (e.g., as a model for the membrane-spanning part of intrinsic membrane proteins) (Killian, 1992) and is currently the best characterized transmembrane peptide. Gramicidin A and its influence on membrane structure have been widely studied using fluorescence, NMR, ESR, DSC, CD, IR, Raman, and X-ray diffraction methods. For example, gA generally increases chain order and reduces both rotational and translational diffusion rates in the interior of liquid-crystalline phospholipid membranes (Cox et al., 1992; Koeppe, Killian & Greathouse, 1994; Patyal, Crepeau & Freed, 1997), though these perturbations of the bilayer structure depend slightly on the conformation of gA (Muller, van Ginkel & van Faassen, 1995). These membrane properties are expected to strongly affect molecular permeability across biomembranes (Xiang & Anderson, 1997 and 1998).

This study is the first of a series of investigations on the effects of transmembrane proteins on molecular transport across model biomembranes. In this study, we have explored the permeabilities of a series of neutral and ionized permeants, α-X-*p*-methyl-hippuric acids (XMHA, X = H, OCH_3, CN, OH, COOH, and $CONH_2$) across egg lecithin bilayers with 10 mol% gA incorporated predominantly in a nonchannel conformation. Because of this nonchannel conformation of gA and the relatively large size of the XMHA permeants employed, the permeabilities obtained are exclusively basal permeabilities the magnitudes of which, however, may be altered due to changes of membrane structure (e.g., local order) or due to the potential existence of an additional permeation pathway along the protein/lipid interface in the presence of gA. The permeability results were used to generate functional group contributions to the transfer of permeant from water to the barrier domain. Linear free-energy relationships were developed between these results and data for solute partition coefficients from water into four distinctive organic solvents (decadiene, chlorobutane, butyl ether, octanol) in order to characterize changes in the chemical selectivity of the transport barrier in the presence of gA. The series of XMHA analogues were chosen because their polar substituents (X) are sufficiently isolated to preclude the possibility of intramolecular hydrogen bonding. The use of polar sub-

stituents as probes of barrier environment is necessary as more lipophilic probes such as -CH_2- groups in a parent permeant molecule often fail to distinguish between nonpolar and polar, hydrogen bonding solvent environments (Orbach & Finkelstein, 1980; Walter & Gutknecht, 1986). The presence of an ionizable carboxylic group in the XMHA analogues allowed permeability coefficients varying over roughly 5–6 orders of magnitude to be determined in the efflux transport experiments by selecting a suitable pH "window" for each permeant so that fluxes were in a detectable range.

Apart from the fundamental importance of understanding the transport of ionizable molecules (e.g., fatty acids and peptide derivatives) across biomembranes, the prediction of their permeation rates across biomembranes would also be particularly useful in drug development. Solute ionization can alter the permeation rate across biomembranes often by several orders of magnitude, potentially accompanied by changes in the transport mechanism. In addition to the commonly assumed mechanisms of ionizable permeant transport via aqueous pores or by solubility and diffusion of the neutral species through the lipid bilayer matrix (Paula et al., 1996, 1998), other transport mechanisms have been invoked to rationalize the passive diffusion of ions, including the net movement of H^+/OH^- along strands of water molecules extending into the membranes via rearrangements of hydrogen bonds (Nichols et al., 1980), transmembrane migration of Cl^- ions assisted by the "flip-flop" of lipid molecules (Toyoshima & Thompson, 1975), the formation of ion pairs in the membrane interior (Riddell & Zhou, 1994), and the formation of deep, asymmetric thinning defects in the bilayer whereby water and polar lipid head groups penetrate the membrane interior to provide a solvation shell for the ion (Wilson & Pohorille, 1996).

Materials and Methods

Materials

L-α-lecithin-(phosphatidylcholine) (>99%) from egg yolk (eggPC) and phosphatidic acid (PA) (>99%) were purchased from Avanti Polar Lipids, (Pelham, AL). Gramicidin A was purchased from Fluka Chemical (Ronkonkoma, NY). All the lipids were stored in a freezer upon arrival. ^{3}H-D-glucose (1 mCi/mL, S.A. 60 Ci/mmol) was obtained from American Radiolabeled Chemicals (St. Louis, MO). The five α-X-*p*-methyl-hippuric acid analogues (X = CN, OCH_3, OH, COOH, and $CONH_2$) shown in Fig. 1 were synthesized in this laboratory as described elsewhere (Mayer, Xiang & Anderson, 2000, *in preparation*). Final purities of these synthesized compounds were >95% by HPLC. *p*-Methyl-hippuric acid (>98%, Sigma Chemical, St. Louis, MO) was used as received without further purification.

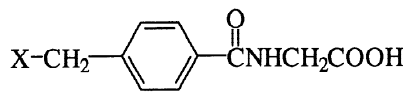

X
-H
-OCH_3
-CN
-OH
-COOH
-$CONH_2$

Fig. 1. Molecular structures of α-X-*p*-methylhippuric acids (XMHA) employed as permeants in this transport study.

Preparation and Characterization of Large Unilamellar Vesicles

Vesicle Preparation

Lipids (50–100 mg eggPC and 3–6 mg PA) were accurately weighed, dissolved in 25 mL chloroform in a test tube, divided into 5–10 aliquots, and evaporated to a dry thin film under nitrogen. A 1.4 mL aliquot of a solution of gramicidin A (1 mM) in ethanol was then added to each sample and the solvent was removed under a stream of nitrogen. The preparation of gA in ethanol is known to incorporate gA into lipid membranes in a predominantly nonchannel conformation (Muller et al., 1995). The dried film was then left under vacuum for 12 hr. A 1 mL aliquot of an aqueous solution containing (1–2) × 10^{-3} M of XMHA permeant (unlabeled) or 10 μCi/mL of radiolabeled α-glucose, 0.01 M buffer (citric acid, phosphate, Tris-HCl, or carbonate), 0.0–0.5 M NaCl, and 0.02 mM EDTA at a given pH was then added to a final total lipid concentration of 10 mg/mL. The dried lipid-protein film was hydrated by repeated vortexing and shaking. The suspension formed was then extruded successively through 0.4, 0.2 and 0.1 μm polycarbonate filters (Nuclepore, Pleasanton, CA) to form large unilamellar vesicles (LUVs). A small amount of negatively charged PA (5 mol%) was included in these membranes to reduce the rate of vesicle aggregation and increase vesicle stability (Cevc et al., 1988).

Dynamic Light Scattering

Vesicle hydrodynamic diameters, *d*, were determined in each vesicle preparation by dynamic light scattering (DLS) measurements. The apparatus for DLS experiments consisted of a goniometer/auto correlator (Model BI-2030AT, Brookhaven, Holtsville, NY) and an Ar^+ ion laser (M95, Cooper Laser Sonics, Palo Alto, CA) operated at 514.5 nm wavelength. Approximately 30 μL of LUV suspension was placed in a clean glass test tube (13 × 75 mm) and diluted to 2 mL with the same filtered buffer solution. The sample was placed in a temperature-controlled cuvette holder with a toluene index-matching bath. Autocorrelation functions were determined for a period of 100–500 sec with a 15-30 μsec duration at 90°C and analyzed by the method of cumulants.

Protein Content Analyses

Incorporation of gramicidin A into lipid membranes was demonstrated by the failure to detect a significant amount of gA in the aqueous

filtrate upon ultrafiltration of gA-containing eggPC LUVs. A new analytical method was developed to determine the gA concentration in the membranes. LUVs were lysed and diluted 1:2 in methanol leading to clear samples which were analyzed for gA by measuring absorption at 280 nm (Cary 3E UV-Vis Spectrophotometer, Varian) using a standard curve of gramicidin A in methanol/water (1:2 v/v) and for phosphorus content by the method of Bartlett (1959).

Circular Dichroism Spectroscopy

The channel and nonchannel conformations of gramicidin A were determined by CD spectroscopy in the wavelength range of 210–260 nm. The CD spectra were obtained on a Jasco Model J-720 Spectropolarimeter (Jasco Spectroscopic, Hachioji City, Japan) with a water-cooled Xenon lamp light source and a path length of 1 cm with computer-controlled data acquisition and analysis. Vesicles with or without gA (for baseline measurements) were prepared at a lipid concentration of 0.5 mM by extrusion through 0.2–0.03 μm polycarbonate filters.

Determination of Permeability Coefficients

Permeant efflux from LUVs was monitored to obtain the permeability coefficient. The experimental procedure included the following steps:

Gel Filtration

A size-exclusion column packed with Sephadex G-50 (medium fractionation range, Sigma) in a 10 mL disposable syringe was equilibrated at 25°C with the same buffer solution as that used to prepare the LUVs but without permeant. Aliquots (0.5–0.6 mL) of the permeant loaded LUVs prepared above were transferred onto the column and eluted by centrifugation (Model CL, IEC, Needham Hts., MA) at two speeds (2 min at 300 × *g*; 1 min at 900 × *g*). The pH of the eluent was monitored to make sure that the eluent pH and that in the original LUV sample were identical. Vesicles with entrapped permeant appeared in the void volume of the size-exclusion column and were well separated from the extravesicular permeant fraction. HPLC analyses of initial and equilibrium extravesicular permeant concentrations in the LUVs indicated an initial ratio of the entrapped to extravesicular permeant concentration after size-exclusion chromatography on the order of 10^5. The eluted LUVs were collected in a screw-capped 10-mL glass vial which was immediately placed in a 25°C water bath.

Ultrafiltration

The concentration gradient created by gel filtration resulted in a net flux of permeant across the LUVs and a continuous increase in the permeant concentration outside the LUVs with time. To determine the flux, aliquots (0.4 mL) of the LUVs after the gel filtration were taken at various time intervals and loaded onto a Centricon-100 filter (MWCO = 100,000; Amicon, Beverly, MA). The loaded sample was then centrifuged at 1,200 × *g* for 3–6 min. The effects of permeant binding to the Centricon-100 filter on filtrate concentrations were examined with selected permeants and at several different permeant concentrations. No significant binding was detected after new filters were preconditioned by rinsing with deionized water. Permeant concentrations in the collected filtrate (*ca.* 100–200 μl) were subsequently analyzed by HPLC for α-X-*p*-methyl-hippuric acids or by liquid scintillation counting (Beckman LS1801, Beckman, Fullerton, CA) for ^{3}H-glucose after 100 μl of the filtrate was mixed with 3 mL of a scintillation cocktail (Aquasol, Opti-Fluor, Packard Instrument, Meriden, CT). Total permeant concentrations in the LUVs were determined by lysing samples with a small amount of Triton X-100 (Sigma) prior to analysis.

The extravesicular permeant concentration due to permeant transport across LUVs varies with time according to the following kinetic equation

$$ln\ (C_\infty - C_0)/(C_\infty - C_t) = k_{obs}\ t \quad (1)$$

where C_0, C_t, and C_∞ are the extravesicular permeant concentrations at time 0 and t, and at equilibrium, respectively, and k_{obs} is the apparent first-order rate constant. The apparent permeability coefficient P_{app} can be obtained from the first-order rate constant, k_{obs}, via the equation

$$P_{app} = k_{obs}V/A \quad (2)$$

where the ratio between the entrapped volume and surface area of the LUVs, V/A, is obtained from the vesicle hydrodynamic diameter, d ($V/A = d/6$).

HPLC Analyses

An HPLC system consisting of a syringe-loaded sample injector (Rheodyne Model 7125, Rainin Instrument, Woburn, MA), a solvent delivery system (110B, Beckman Instruments, San Ramon, CA) operated at a flow rate of 1.0–1.3 mL/min, a dual-wavelength absorbance detector (Model 441, Water Associates, Milford, MA) operated at 254 nm, an integrator (Model 3392A, Hewlett-Packard, Avondale, PA), and a reversed-phase column packed with 5 μm Jupiter RP-C18 (Phenomenex, Torrance, CA) was used at ambient temperature for the analyses of the samples taken during the transport and partitioning experiments. Acetonitrile:water mobile phases buffered to a pH of 3.0 using 0.01 M phosphate buffer and varying from 7 to 30% organic solvent depending on the analyte lipophilicity were employed.

Results and Discussion

Preliminary studies indicated that permeability coefficients for the most polar permeant in the series, α-carbamoyl-*p*-methylhippuric acid, increased systematically with an increase in gramicidin A concentration up to 10 mol % (*data not shown*). Given that a gramicidin concentration of 10 mol% has been the choice in many previous studies of lipid-gramicidin interactions and their effects on membrane structure (e.g., Cox et al., 1992; Muller et al., 1995, 1996), this concentration was also chosen for the present study. Since liposomes with a high protein content tend to be less stable, a small amount of negatively charged PA (5 mol%) was included in these membranes to reduce the rate of vesicle aggregation and increase vesicle stability (Cevc et al., 1988). Dynamic light-scattering results indicated that most vesicle samples prepared in this manner maintained a constant hydrodynamic diameter of approximately 190 nm over an incubation time of at least 10 days.

Conformation of Gramicidin A in Lipid Membranes

Displayed in Fig. 2 are CD spectra of egg lecithin vesicles in the presence of gramicidin A. The appear-

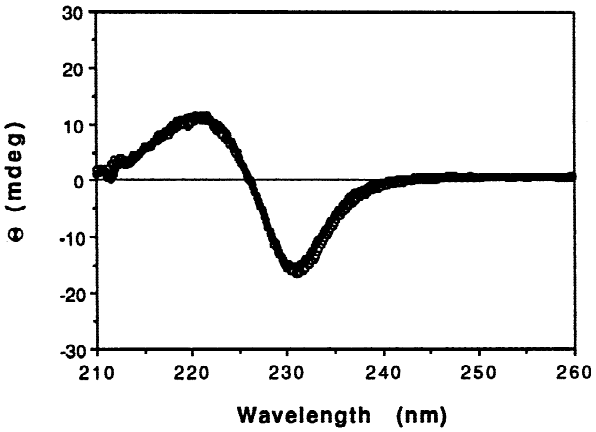

Fig. 2. Circular dichroism spectra for gramicidin A in eggPC/PA vesicles. Gramicidin A was incoporated from ethanol yielding the nonchannel conformation, having a minimum ellipticity at approximately 230 nm. The open and closed circles represent measurements taken 2 hr and 240 hr after the sample preparation.

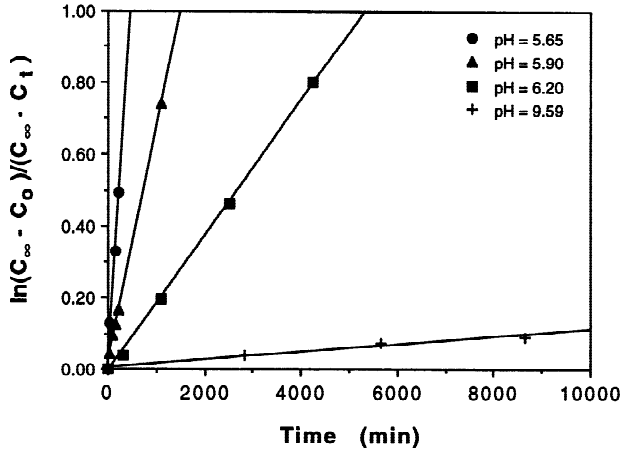

Fig. 3. First-order flux profiles for α-carboxy-*p*-methylhippuric acid across eggPC/gA membranes at different pH values.

ance of a minimum at approximately 230 nm and the absence of a positive maximum ellipticity near 240 nm are characteristics of gramicidin A in a nonchannel conformation (Cox et al., 1992; Muller et al., 1995). Gramicidin A in the nonchannel conformation undergoes a transition to a channel conformation at a high temperature (Tournois et al., 1987; Cox et al., 1992; Killian, 1992). The stability of the non-channel conformation under the experimental conditions employed in the transport studies (25°C) can be assessed by observing the CD spectra taken 2 and 240 hr after the sample preparation. As shown in Fig. 2, the CD spectrum is barely changed after 10 days' incubation, suggesting that the nonchannel conformation remained intact during the time frame of the transport experiments.

pH Dependence of Model Permeant Transport in EggPC/gA Bilayers

Molecular transport across biomembranes is generally attributed to one of two possible pathways (Stein, 1986; Priver, Rabon & Zeidel, 1993; Xiang & Anderson, 1994*b;* Paula et al., 1996): diffusion through transient aqueous pores or solubility-diffusion through a lipid matrix. If the former mechanism dominates, solute permeability would be expected to be molecular size dependent but essentially independent of solute lipophilicity according to a simplified model by Hamilton and Kaler (1990),

$$P_m = \frac{D_w \gamma n_0 RT}{R_v A k_1} [\pi r^2 + RT/k_1] \exp^{(-k_1 \pi r^2 + \epsilon_d)/RT} \qquad (3)$$

where D_w is the diffusion coefficient of permeant in water; γ is the surface concentration enhancement factor due to electrical double layers at the lipid-water interface; A is the membrane surface area, R_v is the mean vesicle radius; R is the gas constant; T is temperature; n_0 is the number of water pores; and r is the permeant radius (unhydrated). The terms $k_1 \pi r^2$ and ϵ_d reflect the energy associated with the formation of a pore of radius r and depth d. The only parameter that is sensitive to the permeant charge is γ. Hamilton and Kaler (1990) assigned a γ value of 10 for cations in synthetic membranes containing negatively charged headgroups. Accordingly, a factor of 0.1 may apply for anions. The γ value can be estimated from the Gouy-Chapman theory (Gouy, 1910; Chapman, 1913). For the membranes used in our study which contain only a small amount (5 mol%) of negatively charged phosphatidic acid, the γ parameters for single-and double-ionized anions are estimated to be 0.49 and 0.24, respectively. Thus, the aqueous pore model would predict a maximum reduction in permeability of a factor of 4 upon solute ionization accompanying changes in solution pH, providing that the barrier properties of the membrane remain roughly constant with varying solution pH.

In contrast to the above prediction, changes of several orders of magnitude were observed in the apparent permeability coefficients of XMHAs with solution pH. Figure 3 shows flux profiles for one of the permeants (α-carboxy-*p*-methyl-hippuric acid, X = COOH) across eggPC/gA membranes at several pH values. As is evident in the linearity of these plots, the fluxes follow closely the kinetic model in Eq. 1 reflecting stable membrane transport properties within the time domain of interest. Solute flux depends strongly on solution pH, being very low at a high pH of 9.6 and several orders of magnitude larger when solution pH is lowered to pH $\leq$ 6.3.

The apparent permeability coefficients obtained ac-

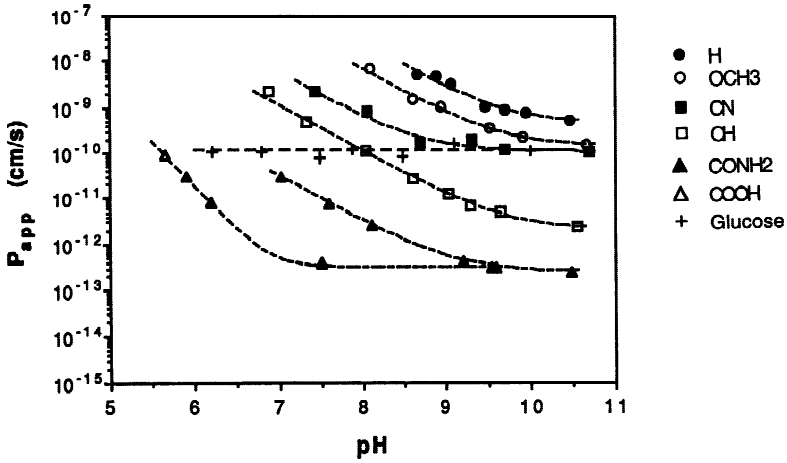

Fig. 4. Apparent permeability coefficients versus pH for α-X-*p*-methylhippuric acids and α-D-glucose across eggPC/gA membranes. The solid curves are generated by nonlinear least-squares fits according to Eqs. 4–6. The dashed line for glucose indicates its average permeability coefficient.

cording to Eq. 2 for all compounds in the series of α-X-*p*-methyl-hippuric acids are plotted in Fig. 4 as a function of pH. In every case the apparent permeability coefficients decrease with increasing solution pH approaching plateau values at a high pH (>10.0) where virtually all of the permeants are ionized and their P_{app} values are extremely small (<5 × 10^{-10} cm/sec). To assess the dependence of membrane barrier properties on solution pH, the permeability coefficient (P_{app}) for α-D-glucose across eggPC/gA membranes was also determined over the pH range of interest as glucose is not ionizable within the pH range explored and any systematic change of glucose's P_{app} with pH would reflect an alteration of bilayer barrier properties with pH. As shown in Fig. 4, the permeability coefficient for glucose is independent of solution pH within experimental error. The value obtained, ~1.2 × 10^{-10} cm/sec, is approximately 4-fold larger than that in protein-free eggPC membranes (Xiang, Xu & Anderson, 1998). The above results thus suggest that at least for all the weak acids used here and in the pH range (<9.0) where P_{app} varies strongly with pH, transport proceeds primarily through the membrane lipid matrix rather than through transient water pores.

If molecular transport is governed by the solubility-diffusion pathway, the neutral (HA) and ionized (A) species should exhibit substantially different permeabilities because of their sharply differing lipophilicities. The pH dependence of the apparent permeability coefficient thus reflects the relative fractions of permeant in neutral and ionized forms, as governed by the acid dissociation constant, K_a. In the absence of unstirred water layer effects (negligible for the vesicles employed in this study) and assuming the barrier properties of the bilayer to be pH independent, as established in Fig. 4, the apparent permeability coefficient P_{app} can be expressed as

$$P_{app} = f_{HA}P^{HA} + (1 - f_{HA})P^{A} \tag{4}$$

where P^{HA} and P^{A} are the intrinsic permeability coefficients for the neutral and ionized species, respectively. The fraction of neutral species, f_{HA}, is

$$f_{HA} = \frac{1}{1 + K_a/[H^+]} \tag{5}$$

or

$$f_{HA} = \frac{1}{1 + K_{a1}/[H^+] + K_{a1}K_{a2}/[H^+]^2} \tag{6}$$

for a monocarboxylic acid or a dicarboxylic acid, respectively. The dissociation constants K_a for the series of XMHA analogues were determined previously (Mayer et al., 2000, *in preparation*). According to Eqs. 4–6, at low pH where $[H^+] \gg K_a$ (or K_{a1} and K_{a2} for α-carboxy-*p*-methylhippuric acid), f_{HA} approaches one and P_{app} reaches a plateau value of P^{HA}. At high pH, f_{HA} becomes negligible and P_{app} approaches a limiting value of P^{A}. At intermediate pH values, where $[H^+] \ll K_a$ (or K_{a1} and K_{a2} for the dicarboxylic acid) but $f_{HA}P^{HA}$ is still much greater than $(1 - f_{HA})P^{A}$, $P_{app} \approx P^{HA}[H^+]/K_a$ ($P_{app} \approx P^{HA}[H^+]^2/K_{a1}K_{a2}$ for the dicarboxylic acid), and logP_{app} is linearly dependent on pH with a slope of −1 or −2. The curves shown in Fig. 4, which represent nonlinear regression analyses of the data according to Eqs. 4–6, indicate that this model can satisfactorily describe the P_{app} − pH profiles generated. For the dicarboxylic acid, the slope of twice that for the other sets is the direct result of the presence of two ionizable carboxyl groups in this solute molecule. A consequence of this greater slope is that the plateau reflecting ion transport occurs at a lower pH. The permeability coefficients for six neutral and ionized XMHA analogues across gA-containing eggPC bilayers obtained from the nonlinear fits are summarized in Table 1 along with those across gA-free eggPC bilayers obtained previously (Mayer et al., 2000, *in preparation*).

Table 1. Permeability coefficients (cm/sec) for neutral and ionized α-X-*p* methyl-hippuric acid analogues across eggPC membranes in the absence and presence of 10 mol% gramicidin A at 25 °C[a]

Permeant	X	EggPC + 10% gA			EggPC[b]
		Neutral species	Ionized species	Ratio[c]	Neutral species
a	–H	$(4.6 \pm 0.5) \times 10^{-4}$	$(4.4 \pm 1.5) \times 10^{-10}$	$(9.6 \pm 2.1) \times 10^{-7}$	$(4.9 \pm 0.4) \times 10^{-4}$
b	$-OCH_3$	$(2.0 \pm 0.2) \times 10^{-4}$	$(1.5 \pm 0.2) \times 10^{-10}$	$(7.5 \pm 1.8) \times 10^{-7}$	$(1.0 \pm 0.1) \times 10^{-4}$
c	–CN	$(1.8 \pm 0.2) \times 10^{-5}$	$(9.6 \pm 0.2) \times 10^{-11}$	$(5.3 \pm 0.7) \times 10^{-6}$	$(9.2 \pm 1.0) \times 10^{-6}$
d	–OH	$(3.1 \pm 0.3) \times 10^{-6}$	$(2.2 \pm 0.4) \times 10^{-12}$	$(7.1 \pm 1.7) \times 10^{-7}$	$(5.5 \pm 0.4) \times 10^{-7}$
e	–COOH	$(5.1 \pm 0.1) \times 10^{-7}$	$(3 \pm 1) \times 10^{-13}$	–	$(1.7 \pm 0.4) \times 10^{-7}$
f	$-CONH_2$	$(8.4 \pm 0.2) \times 10^{-8}$	$(2 \pm 1) \times 10^{-13}$	–	$(9.9 \pm 0.6) \times 10^{-9}$

[a] Expressed as mean ± SD.
[b] Determined from previous experiments using the same transport method (Mayer et al., 2000, *in preparation*).
[c] The ratio of the permeability coefficients for the corresponding ionic and neutral species in eggPC + 10% gA membranes.

As shown by the permeability data in Table 1, a single carboxylic ionization generally decreases the intrinsic permeability by 5–6 orders of magnitude. The presence of two ionized carboxylates in the α-carboxyl substituted MHA also results in a decrease of approximately 6 orders of magnitude in comparison to the neutral species, whereas a decrease of 10–12 orders of magnitude would be expected (barring a change in mechanism) since the two –COOH groups in the permeant are well separated and therefore should exert independent and additive contributions to the free energy of transfer into the membrane. Furthermore, the ionized form of α-carbamoyl-*p*-MHA has a permeability coefficient very close to that for the double ionized α-carboxy-p-MHA. Apparently there is a minimum permeability for these solutes regardless of their lipophilicities. Two mechanisms may be responsible for this behavior. First, for very impermeable solutes such as the doubly ionized form of α-carboxy-p-MHA, permeation through transient water pores, which depends only weakly on solution pH as described earlier, may become significant. Indeed, membrane transport of small cations such as hydrogen and potassium ions may proceed mainly through transient water pores (Paula et al., 1996). Second, the permeability measurement may be limited by a slow rupture/leakage of LUVs due possibly to a slow transition from a bilayer phase to a nonbilayer H_{II} phase (Cox et al., 1992; Tournois et al., 1987) and/or intervesicle interaction (fusion).

Referring to Fig. 4 and Table 1, it is evident that except for the two least permeable ions, the doubly ionized α-carboxy and α-carbamoyl-*p*-MHA anion, solute permeability varies substantially with the nature of the substituent X and the variations are similar in magnitude (i.e., spanning a range of 1–6 orders of magnitude) for both the ionized and neutral species, indicating that both the ionized and neutral species follow pathways that discriminate similarly between permeants on the basis of their lipophilicity. Recent studies by Paula et al. (1998) also found that permeation of halide anions through phospholipid membranes occurs by the solubility-diffusion mechanism even though the halide anions are smaller in size and thereby their transport through transient water pores would be more favorable than the ionic species used in this study. The above results further support the conclusion that the transport of most neutral and ionized α-X-*p*-MHA analogues occurs through a lipid pathway.

Transport Mechanisms for Ionized Permeants

The transport of ionized XMHA analogues may proceed through an electrically silent mechanism involving ion pairs between $XMHA^-$ (abbr. A^-) and cations M^+ as illustrated in Fig. 5*A*, as the formation of ion pairs is expected to cause a substantial reduction in the energy barrier for ion transport. To explore this possibility, the transport of *p*-methylhippuric acid (MHA) across gA-containing eggPC membranes at different NaCl or KCl concentrations was investigated at a high pH ($=10.5$) where the permeability-pH profile has reached a plateau value (*cf.*, Fig. 4). The results are displayed in Fig. 6. Increases in the apparent permeability occur for MHA with increasing $[Na^+]$ or $[K^+]$ approaching a plateau at high cation concentration (>0.5 M). Since the cation concentrations employed (0.05–0.5 M) exceed the permeant concentration (2×10^{-3} M), the apparent permeability P_{app} can be expressed, according to the ion pair transport mechanism, as

$$P_{app} = P^{MA} \frac{K_f[M^+]}{1 + K_f[M^+]} \tag{7}$$

where P^{MA} is the intrinsic permeability coefficient for the ion pair MA and K_f is the formation constant of the ion pair in aqueous solution. Least-squares fits of the permeability data according to Eq. 7 yielded formation con-

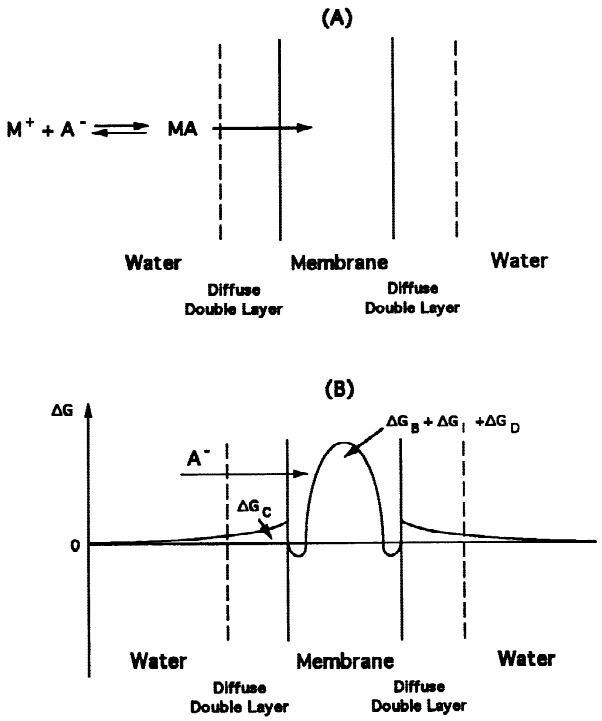

Fig. 5. Schematic depiction of the effects of various electrostatic interaction components (*see* text for definitions) on transport of ionized permeants A^- in the form of ion pairs MA (panel *A*) and the transport of anions (panel *B*).

stants of $K_f = 17 \pm 4\ \text{M}^{-1}$ and $19 \pm 9\ \text{M}^{-1}$ for the ion pairs NaA and KA, respectively, suggesting that at a salt concentration of 0.1 M, the condition used in most of the transport experiments, more than half of the ionized MHA would exist as an ion pair in solution. The similarities in both K_f and the plateau value in the presence of either Na^+ and K^+ imply that both the formation of ion pairs and the partitioning of ion pair into the membrane interior are independent of the chemical nature of the cations employed (Na^+ *vs.* K^+) if the ion-pair mechanism dominates. While ion pair formation constants between carboxylic acids and alkali metal ions are scarce in the literature, a relatively strong dependence of the formation constants for acetate on cation size has been reported previously (e.g., K_f for LiA and NaA are 1.8 and 0.66, respectively (Sillen & Martell, 1971)).

Changes in salt concentration may also alter the surface electrostatic potential (Ψ_o) between the membrane interface and the bulk aqueous solution caused by the presence of negatively charged PA lipids in the membranes. This negative surface potential disfavors the permeation of anions, resulting in a positive contribution to the free energy of transfer of ionized permeants as shown in Fig. 5*B*. The presence of indifferent cations in solution would partly shield permeating anions to the electric field generated by the surface charge. This can be described by the Gouy-Chapman theory of the diffuse double layer (Gouy, 1910; Chapman, 1913), in which the relation between the surface potential (Ψ_o) and the aqueous electrolyte concentration $[M^+]$ can be expressed as

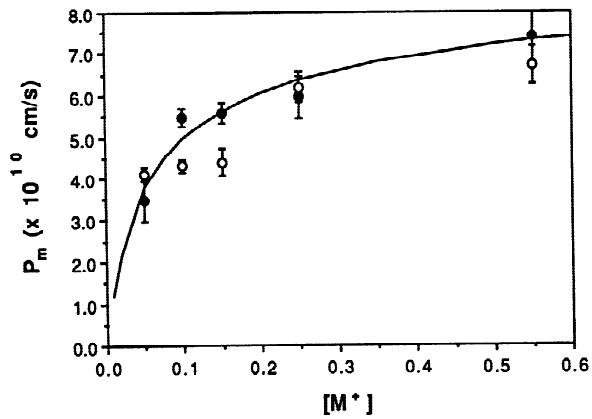

Fig. 6. Apparent permeability coefficients for *p*-methylhippuric acid across eggPC + 10 mol% gA membranes at pH = 10.5 as a function of $[Na^+]$ (solid circles) or $[K^+]$ (open circles).

$$\frac{\sigma}{(8N\epsilon_r\epsilon_o kT[M^+])^{1/2}} = \sinh(e\psi_o/2kT) \tag{8}$$

where σ is the surface charge density, N is Avogadro's constant, ϵ_r is the dielectric constant, ϵ_o is the permittivity of free space, k is the Boltzmann constant, T is temperature, and e is electronic charge. The contribution of this surface potential to the permeability of ionic solutes P^A can then be written as

$$P^A = P_o^A e^{-ze\Psi_o/kT} \tag{9}$$

where P_o^A is the permeability in the absence of a surface potential ($\Psi_o = 0$) and is independent of the aqueous electrolyte concentration. z is the valence of the ionized permeant. The solid curve in Fig. 6 shows a least-squares fit according to Eqs. 8 and 9, which yields $P_o^A = (9.7 \pm 0.9) \times 10^{-10}$ cm/sec and a surface charge density of 4.7 mol% ($r = 0.97$). This is very close to the concentration (5 mol%) of the negatively charged *PA* lipids used in these experiments. This electrically active mechanism is also independent of the nature of the cation, consistent with the permeability results in Fig. 6, suggesting that the transport of ionized MHA analogues across eggPC/gA membranes may proceed through an electrically active mechanism rather than in the form of neutral ion pairs. Ion-pair formation was also not considered to be the dominant mechanism for permeation of halide anions through phospholipid membranes (Paula et al., 1998).

The strong effects of molecular ionization on permeability are manifested by the ratio of the permeability coefficients for the ionized and neutral XMHA ana-

logues as listed in Table 1. As noted, the permeability ratio varies within a narrow range of $7 \times 10^{-7} - 5 \times 10^{-6}$. It is interesting to compare these results with the transport data available in the literature. Previous studies of the transport of HCl and Cl^- across phospholipid membranes (Gutknecht & Walter, 1981; Paula et al., 1998) have yielded a permeability ratio P_{Cl^-}/P_{HCl} of ~1×10^{-9}, which is 3–4 orders of magnitude smaller than the present results for XMHA analogues. Two factors may be responsible for this large difference. First, the negative charge present in an ionized XMHA molecule is delocalized due to conjugation within the $-COO^-$ group and induction by the adjacent polar atomic groups increasing the effective ionic radius, and second, the barrier domain in gA-containing eggPC membranes may be less hydrophobic, with a higher relative dielectric constant ϵ_m than in eggPC membranes without gramicidin A (*vida infra*). Among various solvation energy components that may be altered by both ionic radius (r) and membrane dielectric constant (ϵ_m) are the Born (ΔG^o_B) and image (ΔG^o_I) solvation energies (Parsegian, 1969)

$$\Delta G^\circ_B + \Delta G^\circ_I = \frac{e^2}{4\pi\epsilon_o}\left[\frac{1}{2r}\left(\frac{1}{\epsilon_m} - \frac{1}{\epsilon_w}\right) - \frac{1}{\epsilon_m d}\, ln\left(\frac{2\epsilon_w}{\epsilon_w + \epsilon_m}\right)\right] \tag{10}$$

From the above equation, it is thus clear that increases of r and ϵ_m tend to lower the solvation free energy which the ionized XMHAs must overcome in order to penetrate through the membrane.

The transport of ionized XMHAs across membranes may also be limited by the requirement of electroneutrality in the adjacent aqueous solutions both inside and outside the vesicles. To maintain electroneutrality there must be either a flux of cations in the same direction, an equivalent flux of anions in the opposite direction, or a combination of the two, with respect to the flux of the ionized species of interest. The existence of a plateau region for P^A *vs.* pH at a high pH suggests that H^+ cotransport is not the source of ions responsible for maintaining electroneutrality. Other ionic species such as OH^- and Na^+ have permeabilities 1–2 orders smaller than that for H^+ (Nichols et al., 1980; Gutknecht & Walter, 1981), but because of their much larger concentrations at pH = 9, their fluxes are on the order of 10^{-16} – 10^{-18} mole/cm^{2}sec, comparable to those for ionized XMHA analogues.

Nature of the Transport Barrier Domains in eggPC/gA Bilayers

If molecular permeation is governed by the solubility-diffusion mechanism, the overall membrane resistance to solute permeation, defined as the inverse of the permeability coefficient, P_m, can be expressed as the integral over the local resistances across the membrane (Diamond, Szabo & Katz, 1974),

$$\frac{1}{P_m} = \int_0^d \frac{dz}{K_{z/w} D_z} \tag{11}$$

where $K_{z/w}$ and D_z are the depth-dependent partition coefficients from water into the membrane and the diffusion coefficient for the permeating solute in the membrane at position z, respectively, and d is the entire membrane thickness, including the membrane/water interfaces. For ionic species such as $XMHA^-$ analogues, the partition coefficient $K_{z/w}$ depends on the membrane potential due to the interfacial polarization (ΔG_I), interfacial charge (ΔG_C) and dipole distributions (ΔG_D) (Flewelling & Hubbell, 1986), but these free energy components can be considered, to a first-order approximation, independent of the nature of the neutral substituent X in the MHA compounds. Thus, the partition coefficient ($K_{z/w}$) is related to the intrinsic partition coefficient $K'_{z/w}$, which is defined as the partition coefficient between two thermodynamic phases free of the interfacial effects, by

$$K_{z/w} = K'_{z/w} e^{-(\Delta G^\circ_I + \Delta G^\circ_C + \Delta G^\circ_D)/kT} \tag{12}$$

The permeability model in Eq. 11, which takes into account the heterogeneous nature of biomembranes, can be simplified to

$$P_m = \frac{K_{b/w} D_b}{d_b} \tag{13}$$

if the overall resistance, $1/P_m$, is determined disproportionately by the resistance in a distinct region (i.e., the barrier domain) within the membrane. In Eq. 13, $K_{b/w}$ and D_b are the corresponding partition and diffusion coefficients in this barrier domain, respectively, and d_b now represents the thickness of the barrier domain. Indeed, computer simulations by Marrink and Berendsen (1994; 1996) have demonstrated distinct permeability properties in different regions of lipid membranes. Since the series of XMHA compounds listed in Fig. 1 are similar in molecular size and shape and therefore are likely to exhibit similar diffusion and excluded-volume partition properties within biomembranes (Xiang & Anderson, 1994a; Schnitzer, 1988), their inherent lipophilicities as represented by $K'_{b/w}$ become the predominant determinants of their relative permeability coefficients. Unfortunately, $K_{b/w}$ (or $K'_{b/w}$) cannot be obtained from direct membrane/water partition experiments as a solute tends to partition into that region with the lowest solvation energy rather than into the barrier domain where the solvation energy is the highest (i.e., least favorable). Consequently, to identify the barrier domain in biomembranes,

one needs to search for a model solvent system which best describes the hydrophobicity of the barrier domain.

To identify this model solvent, we rely on the linear free energy principle that correlates the solvation free energies for a series of solutes (RX) in one solvent with the corresponding values in another solvent of similar physicochemical properties (Collander, 1951).

$$logK^{RX}_{org_2/w} = s\ logK^{RX}_{org_1/w} + c \tag{14}$$

The slope, *s*, often referred to as the selectivity coefficient (Katz, Hoffman & Blumenthal, 1983), measures the similarity of these two solvents with respect to their affinities for the solute series. An *s* of one indicates that two solvents have identical selectivities and therefore similar hydrophobicities. As discussed earlier, the relative membrane permeabilities of a series of similarly sized solutes such as the series of XMHA analogues are determined mainly by their relative intrinsic partition coefficients into the barrier domain. Thus, one can also develop a linear free-energy relationship between P_m and $K_{org/w}$ for the series of XMHA analogues,

$$logP^{RX}_m = s\ logK^{RX}_{org/w} + c \tag{15}$$

The most suitable model solvent that mimics the barrier domain in biomembranes would then be the one which provides an *s* value of one. For the parent compound RH (X = H), we have

$$logP^{RH}_m = s\ logK^{RH}_{org/w} + c \tag{16}$$

Subtracting Eq. 16 from Eq. 15 and defining $\Delta(\Delta G^\circ_m)_X$ and $\Delta(\Delta G^\circ_o)_X$, the functional group contributions to solute transfer from water into the barrier domain in the membranes and the model organic solvent, respectively, as

$$\Delta(\Delta G^\circ_m)_X = -RT\ ln\ (P^{RX}_m/P^{RH}_m) \tag{17}$$

$$\Delta(\Delta G^\circ_o)_X = -RT\ ln\ (K^{RX}_m/K^{RH}_m) \tag{18}$$

we derive a linear free-energy relationship for the series of functional groups, *X*,

$$\Delta(\Delta G^\circ_m)_X = s\Delta(\Delta G^\circ_o)_X + c \tag{19}$$

This relationship enables us to use the functional group contribution data $\Delta(\Delta G^\circ_o)_X$ obtained from other series of compounds such as α-X-*p*-toluic acids for the correlation analysis. This is necessary as the series of XMHA analogues are relatively hydrophilic and their partition coefficients between water and a nonpolar organic solvent are difficult to obtain accurately.

The solvent characteristics which determine the affinity of a solute for that solvent can be analyzed in terms of polarity/polarizability, usually characterized by the dielectric constant and refractive index, and hydrogen-bond donating/accepting capacities (Kamlet et al., 1988; Marcus, 1991). Biomembranes are unique in that even in the absence of membrane proteins, they exhibit a heterogeneous *trans*-bilayer atomic distribution, reflecting a hydrated headgroup interface, a transition region between the headgroups and acyl chains (the glycerol linkages), and an ordered acyl chain region. Thus, different regions within the membranes may possess markedly different solvent properties. The hydrated headgroup region at the membrane/water interface, for example, resembles a highly polar, hydrogen-bond donating/accepting solvent such as isoamyl alcohol (Diamond & Katz, 1974). The region of the glycerol linkages between the headgroups and the acyl chains is less hydrated but is enriched in hydrogen-bond acceptor groups. The acyl chain region is hydrocarbon-like but its polarizability may be altered by the degree of chain unsaturation and its effective polarity may be increased by its proximity to the hydrated interface. The presence of transmembrane proteins would conceivably alter the solvation characteristics of all these distinctive regions including the barrier domain in the membranes.

Based on the above analysis, four model solvents (decadiene, chlorobutane, butyl ether, and octanol) were chosen to potentially describe the possible contributions of polarizability, polarity, and hydrogen-bond donating/accepting capacity to the barrier microenvironment in phospholipid membranes in the presence of the transmembrane protein gA. Decadiene has two double bonds, thus resembling the lipid acyl chains in eggPC, and is found to mimic closely the barrier environment in eggPC membranes in the absence of transmembrane protein (Xiang & Anderson, 1994*b*). Chlorobutane is relatively polar with a dielectric constant of 7.3, significantly greater than that of nonpolar hydrocarbons (*ca.* 1.9–2.3). These two solvents have negligible hydrogen-bond donating/accepting capacity. Butyl ether has a single oxygen atom which may function as a hydrogen-bond acceptor resembling the glycerol linkages in eggPC and various polar groups in gramicidin A. Octanol, which has the same atomic composition as butyl ether, is capable of both hydrogen-bond donation and acceptance, and is extensively employed as a model solvent for structure-biological activity studies. The substituent contributions to transfer of solute from water into these four organic solvents have been reported previously (Xiang, Xu & Anderson, 1998) and are listed in Table 2 along with those obtained from the permeability coefficients for XMHA analogues in either neutral or ionized form across eggPC membranes in the presence and absence of 10 mol% gA.

Linear free energy relationships (i.e., plots of $\Delta(\Delta G^\circ_m)_X$ *vs.* $\Delta(\Delta G^\circ_o)_X$ for the transfer of neutral

Table 2. Functional group contributions to the molar free energy (cal/mol) of transfer of α-X-*p*-methyl-hippuric acid analogues from water into various membrane barrier domains and model solvents at 25 °C[a]

X	EggPC + 10% gA		EggPC[b]	Decadiene[c]	Chlorobutane[c]	Butylether[c]	Octanol[c]
	HA	A^-					
H	0	0	0	0	0	0	0
OCH_3	515	630	940	1240	1010	900	840
CN	1920	910	2350	2350	1750	1770	1640
OH	2980	3160	4020	4210	4640	2980	2000
COOH	4040	—	4720	5270	5540	2610	1560
$CONH_2$	5120	—	6400	6010	6190	4390	2870

[a] Calculated according to Eqs. 17 and 18.
[b] From (Mayer et al., 2000, *in preparation*).
[c] From (Xiang & Anderson, 1994b; Xiang et al., 1998).

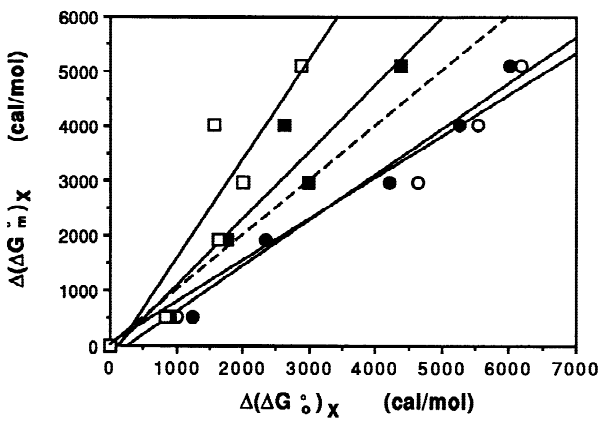

Fig. 7. Linear free energy relationships of the functional group contributions to the transfer of neutral α-X-*p*-methylhippuric acids to the barrier domain in eggPC/gA membranes, $\Delta(\Delta G°_m)_X$, with those to the transfer to various model organic solvents, $\Delta(\Delta G°_o)_X$. A dashed line with a slope of one is also shown for comparison. Key: (●), decadiene; (○), chlorobutane; (■), butyl ether; and (□), octanol.

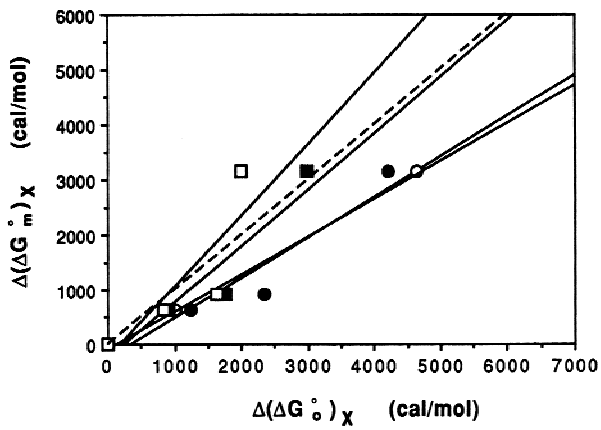

Fig. 8. Linear free-energy relationships of the functional group contributions to the transfer of ionic α-X-*p*-methyl-hippuric acids to the barrier domain in eggPC/gA membranes, $\Delta(\Delta G°_m)_X$, with those to the transfer to various model organic solvents, $\Delta(\Delta G°_o)_X$. A dashed line with a slope of one is also shown for comparison. Key: (●), decadiene; (○), chlorobutane; (■), butyl ether; and (□), octanol.

XMHA analogues from water into the barrier domain in gA-containing eggPC membranes and into the four model organic solvents (octanol, butyl ether, chlorobutane, decadiene) are displayed in Fig. 7. Similar correlations for the ionized XMHA analogues are presented in Fig. 8. The slopes and correlation coefficients generated from linear regression analyses are summarized in Table 3 along with the results for protein-free eggPC membranes obtained in a separate study (Xiang & Anderson, 1994*b*).

The hydrogen-bonding solvent octanol yields slopes substantially greater than one in correlations with eggPC membranes in both the presence and absence of gramicidin A, indicating that regardless of the presence of gramicidin A, the barrier domains in these membranes resemble more closely a nonhydrogen bond donating solvent. It is thus suggested that in both protein-free and protein-containing membranes, the barrier domain for transport does not reside in the hydrated headgroup regions. This result further rules out the involvement of transient water pores in the transport of both neutral and ionized XMHA analogues as these water pores would be expected to be even more hydrophilic than octanol. Also, these results are in sharp contrast to the conclusions of Subczynski et al. (1994) obtained in an ESR spin-labeling study that the solvent properties of phospholipid membranes are alcohol-like (even at the membrane center). It seems that their use of polar spin labels (nitroxides) at various positions in the lipid chains in an attempt to probe the local hydrophobicity may have induced artificially higher water concentrations in the neighborhood of the spin probes. Alternatively, polar spin probes may reside at the bilayer/water interface. The extremely low temperature (−150°C) used in the ESR studies may also have contributed to the differences between their results and those obtained in this study.

Table 3. The slopes (*s*) and correlation coefficients (*r*) for the linear free-energy relationships of functional group contributions between lipid membranes and model solvents according to Eq. 19

Membrane/Permeant	Solvent	*s*	*r*
EggPC + gA/HA	Decadiene	0.83 ± 0.06	0.990
	Chlorobutane	0.75 ± 0.08	0.977
	Butyl Ether	1.22 ± 0.17	0.962
	Octanol	1.84 ± 0.43	0.906
EggPC + gA/A^-	Decadiene	0.74 ± 0.16	0.957
	Chlorobutane	0.69 ± 0.05	0.996
	Butyl Ether	1.02 ± 0.25	0.945
	Octanol	1.29 ± 0.60	0.837
EggPC/HA[a]	Decadiene	0.99 ± 0.04	0.996
	Chlorobutane	0.90 ± 0.04	0.989
	Butyl Ether	1.39 ± 0.19	0.956
	Octanol	2.4 ± 0.5	0.909

[a] Determined from previous experiments using the BLM transport method (Xiang & Anderson, 1994*b*).

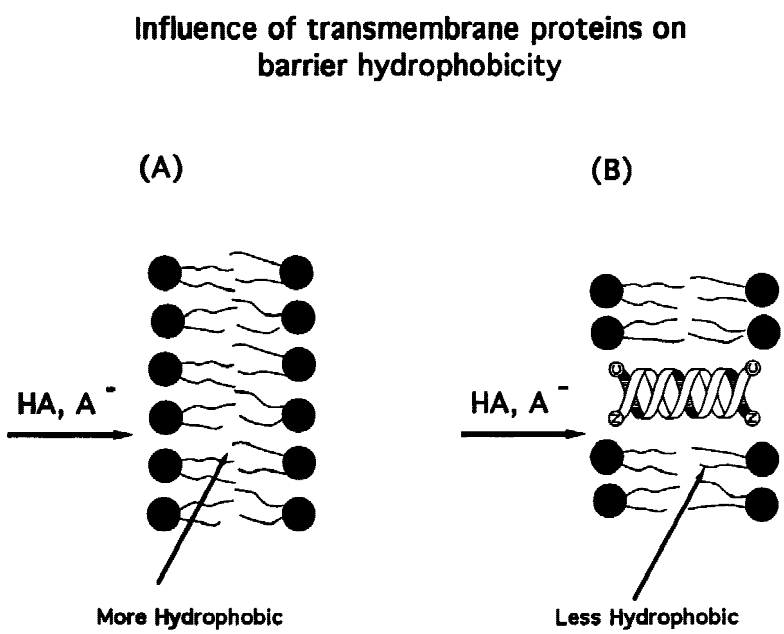

Fig. 9. A schematic depiction of the influence of gramicidin A on the transport barrier domain in a lipid bilayer membrane.

The results in Table 3 also show that the transmembrane protein, gramicidin A, has a substantial influence on the barrier domain selectivity in lipid membranes. In the absence of the transmembrane proteins, the barrier domain in eggPC membranes appears to closely resemble decadiene in its selectivity ($s = 0.99$), while butyl ether and octanol yield much higher slopes (1.4–2.4), indicating that the barrier domain in these membranes resembles a nonpolar, nonhydrogen-bonding solvent with some degree of chain unsaturation. Clearly, the barrier domain resides in the acyl chain region of the membranes where electrostatic interaction is least favorable. With the addition of 10 mol% gA, the slopes become significantly less than 1 (i.e., 0.7–0.8) for correlations with the nonhydrogen bonding solvents (i.e., decadiene and chlorobutane), approaching a value of 1.0–1.2 for correlations with butyl ether. These results suggest that the barrier domain in gA-containing eggPC membranes is more interactive with hydrogen bonding permeants and therefore less selective to permeant structure than the barrier domain in protein-free eggPC membranes. Considered in isolation, these changes in the barrier selectivity could perhaps be ascribed to changes in local polarity in the membranes because decadiene and butyl ether have quite different dipole moments of ca. 0.0 and 1.8 debye units, respectively. However, correlations with chlorobutane yield even smaller slopes despite chlorobutane's higher dipole moment (2.1 debye units). Thus, the differences do not appear to involve membrane polarity. Rather, the barrier domains in gA-containing eggPC membranes appear to possess some degree of hydrogen-bond accepting capacity, which

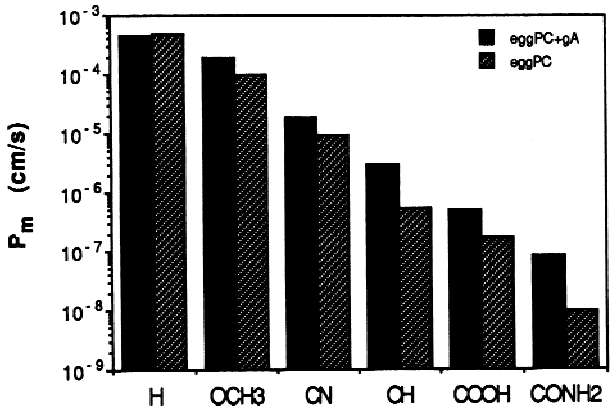

Fig. 10. Comparison of the permeability coefficients for the series of neutral α-X-*p*-methyl-hippuric acids across eggPC membranes in the presence and absence of 10 mol% gramicidin A.

could be rationalized if some of the pathways for permeant diffusion in the membranes are along the interface between lipid chains and the membrane-spanning protein, the surface of which is likely to contain functional groups that are capable of accepting hydrogen bonds from penetrating permeants, as illustrated in Fig. 9.

As shown in Fig. 10, the presence of gramicidin A has a significant and complex effect on molecular permeability. For example, the permeability coefficient for the most lipophilic compound in the XMHA series, *p*-methyl-hippuric acid in gA-containing eggPC membranes is close to that in gA-free eggPC membranes. On the contrary, XMHA analogues with polar, hydrogen-bonding X substituents exhibit permeability coefficients which are 2–8-fold larger in gA-containing eggPC membranes. It appears that the protein effect on permeability is amplified for the more hydrophilic substituents. This is further supported by the 4-fold larger permeability for glucose across gA-containing eggPC membranes ($P_m = 1.2 \times 10^{-10}$ cm/sec) in comparison to gA-free eggPC membranes ($P_m = 3.0 \times 10^{-11}$ cm/sec) (Xiang et al., 1998). The similarity of the permeability values of *p*-methyl-hippuric acid, the most lipophilic compound in the series, across gA-containing and gA-free membranes may reflect a balance of the effects of increased chain ordering in gA-containing membranes (Muller et al., 1995), which decreases permeabilities (Xiang & Anderson, 1997), and the enhancement in transport provided by the presence of hydrogen acceptor functional groups in the gA containing membrane.

In summary, we have found a strong influence of the transmembrane protein gA on permeabilities of neutral and ionized XMHA analogues across egg lecithin membranes. The general trend is that given the same molecular size, the more hydrophilic the permeant, the larger the increase in permeability in the presence of gA. The strong substituent and acid ionization contributions to molecular permeability ($\Delta(\Delta G_m)_X$ = 0–5200 cal/mol and $P^A/P^{HA} = 7 \times 10^{-7} - 6 \times 10^{-6}$) and the saturation behaviors of the effects of indifferent electrolytes to permeabilities of the ionized permeants points to a solubility-diffusion mechanism through the lipid membranes rather than a transport pathway through transient water pores for both the neutral and ionic species. On the basis of a quantitative analysis of the solvent properties in the membranes using the sensitive functional group contribution method and the linear free-energy principle, the origin of this strong influence of the transmembrane protein on permeability is traced to the lowering of the hydrophobicity in the membrane interior likely due to the presence of hydrogen bond acceptor functional groups at the protein-lipid interface within the membrane. Since biomembranes are invariably composed of proteins embedded in a matrix of lipid bilayer, the present revelation of changes of membrane barrier hydrophobicity in the presence of transmembrane proteins and their effects on molecular permeability is believed to be an important and pioneering step towards an accurate prediction of molecular permeability in biomembranes. More investigations are underway to explore the effects of the protein content and conformation on molecular transport across lipid membranes.

This work was supported by a grant from the National Institutes of Health (RO1 GM51347).

References

Anderson, B.D., Higuchi, W.I., Raykar, P.V. 1988. Heterogeneity effects on permeability-partition coefficient relationships in human stratum corneum. *Pharm. Res.* **5:**566–573

Anderson, B.D., Raykar, P.V. 1989. Solute structure-permeability relationships in human stratum corneum. *J. Invest. Dermatol.* **93:**280–286

Anderson, O.S. 1984. Gramicidin channels. *Annu. Rev. Physiol.* **46:**531–548

Bartlett, G.R. 1959. Phosphorous assay in column chromatography. *J. Biol. Chem.* **234:**466–468

Carruthers, A., Melchior, D.L. 1983. Studies of the relationship between bilayer water permeability and bilayer physical state. *Biochemistry* **22:**5797–5807

Cevc, G., Seddon, J.M., Harttung, R., Eggert, W. 1988. Phosphatidylcholine-fatty acid membranes. I. Effects of protonation, salt concentration, temperature and chain length on the colloidal and phase properties of mixed vesicles, bilayers and nonlamellar structures. *Biochem. Biophys. Acta* **940:**219–240

Chapman, D.L. 1913. A contribution to the theory of electrocapillarity. *Philos. Mag.* **25:**475–481

Clerc, S.G., Thompson, T.E. 1995. Permeability of dimyristoyl phosphatidylcholine/dipalmitoyl phosphatidylcholine bilayer membranes with coexisting gel and liquid-crystalline phases. *Biophys. J.* **68:**2333–2341

Collander, R. 1951. The partition of organic compounds between higher alcohols and water. *Acta Chem. Scand.* **5:**774

Cornell, B. 1987. Gramicidin A-phospholipid model systems. *J. Bioenerg. Biomembr.* **19:**655–676

Cox, K.J., Ho, C., Lombardi, J.V., Stubbs, C.D. 1992. Gramicidin conformational studies with mixed-chain unsaturated phospholipid bilayer systems. *Biochemistry* **31:**1112–1118

Diamond, J.M., Katz, Y. 1974. Interpretation of nonelectrolyte partition coefficients between dimyristoyl lecithin and water. *J. Membrane Biol.* **17:**121–154

Diamond, J.M., Szabo, G., Katz, Y. 1974. Theory of nonelectrolyte permeation in a generalized membrane. *J. Membrane Biol.* **17:**148–152

Finkelstein, A. 1976. Water and nonelectrolyte permeability of lipid bilayer membranes. *J. Gen. Physiol.* **68:**127–135

Flewelling, R.F., Hubbell, W.L. 1986. The membrane dipole potential in a total membrane potential model. *Biophys. J.* **49:**541–552

Gouy, M. 1910. Sur la constitution de la charge electrique a la surface d'un electrolyte. *J. Phys.* **9:**457–468

Gutknecht, J., Walter, A. 1981. Transport of protons and hydrochloric acid through lipid bilayer membranes. *Biochim. Biophys. Acta* **641:**183–188

Hamilton, R.T., Kaler, E.W. 1990. Alkali metal ion transport through thin bilayers. *J. Phys. Chem.* **94:**2560–2566

Haydon, D.A., Hladky, S.B. 1972. Ion transport across thin lipid membranes: A critical discussion of mechanisms in selected systems. *Quart. Rev. Biophys.* **5:**187–282

Kamlet, M.J., Doherty, R.M., Abraham, M.H., Marcus, Y., Taft, R.W. 1988. Linear solvation energy relationships. 46. An improved equation for correlation and prediction of octanol/water partition coefficients of organic nonelectrolytes (including strong hydrogen bond donor solutes). *J. Phys. Chem.* **92:**5244–5255

Katz, Y., Hoffman, M.E., Blumenthal, R. 1983. Parametric analysis of membrane characteristics and membrane structure. *J. Theor. Biol.* **105:**493–510

Killian, J.A. 1992. Gramicidin and gramicidin-lipid interactions. *Biochim. Biophys. Acta* **1113:**391–425

Koeppe, R.E., Killian, J.A., Greathouse, D.V. 1994. Orientations of the tryptophan 9 and 11 side chains of the gramicidin channel based on deuterium nuclear magnetic resonance spectroscopy. *Biophys. J.* **66:**14–24

Lande, M.B., Donovan, J.M., Zeidel, M.L. 1995. The relationship between membrane fluidity and permeabilities to water, solutes, ammonia, and protons. *J. Gen. Physiol.* **106:**67–84

Levin, V.A. 1980. Relationship of octanol/water partition coefficient and molecular weight to rat brain capillary permeability. *J. Med. Chem.* **23:**682–684

Marcus, Y. 1991. Linear solvation energy relationships. Correlation and prediction of the distribution of organic solutes between water and immiscible organic solvents. *J. Phys. Chem.* **95:**8886–8891

Marrink, S.J., Berendsen, H.J.C. 1994. Simulation of water transport through a lipid membrane. *J. Phys. Chem.* **98:**4155–4168

Marrink, S.J., Berendsen, H.J.C. 1996. Permeation process of small molecules across lipid membranes studied by molecular dynamics simulations. *J. Phys. Chem.* **100:**16729–16738

Muller, J.M., van Ginkel, G., van Faassen, E.E. 1995. Effect of gramicidin A on structure and dynamics of lipid vesicle bilayers. A time-resolved fluorescence depolarization study. *Biochemistry* **34:**3092–3101

Muller, J.M., van Ginkel, G., van Faassen, E.E. 1996. Effect of lipid molecular structure and gramicidin A on the core of lipid vesicle bilayers. A time-resolved fluorescence depolarization study. *Biochemistry* **35:**488–497

Nichols, J.W., Hill, M.W., Bangham, A.D., Deamer, D.W. 1980. Measurement of net proton-hydroxyl permeability of large unilamellar liposomes with the fluorescent pH probe, 9-aminoacridine. *Biochim. Biophys. Acta* **596:**393–403

Orbach, E., Finkelstein, A. 1980. The nonelectrolyte permeability of planar lipid bilayer membranes. *J. Gen. Physiol.* **75:**427–436

Parsegian, A. 1969. Energy of an ion crossing a low dielectric membrane: solutions to four relevant electrostatic problems. *Nature* **221:**844–846

Patyal, B.R., Crepeau, R.H., Freed, J.H. 1997. Lipid-gramicidin interactions using two-dimensional Fourier-transform electron spin resonance. *Biophys. J.* **73:**2201–2220

Paula, S., Volkov, A.G., Hoek, A.N.V., Haines, T.H., Deamer, D.W. 1996. Permeation of protons, potassium ions, and small polar molecules through phospholipid bilayers as a function of membrane thickness. *Biophys. J.* **70:**339–348

Paula, S., Volkov, G., Deamer, D.W. 1998. Permeation of halide anions through phospholipid bilayers occurs by the solubility-diffusion mechanism. *Biophys. J.* **74:**319–327

Priver, N.A., Rabon, E.C., Zeidel, M.L. 1993. Apical membrane of the gastric parietal cell: Water, proton, and nonelectrolyte permeabilities. *Biochemistry* **32:**2459–2468

Rapoport, S.I., Ohno, K., Pettigrew, K.D. 1979. Drug entry into the brain. *Brain Res.* **172:**354-359

Riddell, F.G., Zhou, Z. 1994. Mn^{2+} as a contrast reagent for NMR studies of 35_{Cl^-} and 81_{Br^-} transport through model biological membranes. *J. Inorg. Biochem.* **55:**279–93

Schnitzer, J.E. 1988. Analysis of steric partition behavior of molecules in membranes using statistical physics. Application to gel chromatography and electrophoresis. *Biophys. J.* **54:**1065–1076

Sillén, L.G., Martell, A.E. 1971. Stability constants of metal-ion complexes. Suppl. 1, The Chemical Society, London

Singer, S.J., Nicolson, G.L. 1972. The fluid mosaic model of the structure of cell membranes. *Science* **175:**720–731

Stein, W.D. 1986. Transport and Diffusion Across Cell Membranes. Academic Press, Orlando

Subczynski, W.K., Lewis, R.N.A.H., McElhaney, R.N., Hodges, R.S., Hyde, J.S., Kusumi, A. 1998. Molecular organization and dynamics of 1-palmitoyl-2-oleoylphosphatidylcholine bilayers containing a transmembrane α-helical peptide. *Biochemistry* **37:**3156–3164

Subczynski, W.K., Wisniewska, A., Yin, J.-J., Hyde, J.S., Kusumi, A. 1994. Hydrophobic barriers of lipid bilayer membranes formed by reduction of water penetration by alkyl chain unsaturation and cholesterol. *Biochemistry* **33:**7670–7681

Tournois, H., Killian, J.A., Urry, D.W., Bokking, O.R., de Gier, J., de Kruijff, B. 1987. Solvent determined conformation of gramicidin affects the ability of the peptide to induce hexagonal H_{II} phase formation in dioleoylphosphatidylcholine model membranes. *Biochim. Biophys. Acta* **905:**222–226

Toyoshima, Y., Thompson, T.E. 1975. Chloride flux in bilayer membranes: The electrically silent chloride flux in semispherical bilayers. *Biochemistry* **14:**1518–1524

Wallace, B.A. 1990. Gramicidin channels and pores. *Annu. Rev. Biophys Biophys. Chem.* **19:**127–157

Walter, A., Gutknecht, J. 1986. Permeability of small nonelectrolytes through lipid bilayer membranes. *J. Membrane Biol.* **90:**207–217

Wilson, M.A., Pohorille, A. 1996. Mechanism of unassisted ion transport across membrane bilayers. *J. Am. Chem. Soc.* **118:**6580–6587

Xiang, T.-X., Anderson, B.D. 1994*a*. Molecular distributions in lipid bilayers and other interphases: A statistical mechanical theory combined with molecular dynamics simulation. *Biophys. J.* **66:**561–573

Xiang, T.-X., Anderson, B.D. 1994*b*. Substituent contributions to the permeability of substituted *p*-toluic acids in lipid bilayer membranes. *J. Pharm. Sci.* **83:**1511—1518

Xiang, T.-X., Anderson, B.D. 1997. Permeability of acetic acid across gel and liquid-crystalline lipid bilayers conforms to free-surface-area theory. *Biophys. J.* **72:**223–237

Xiang, T.-X., Chen, X., Anderson, B.D. 1992. Transport methods for probing the barrier domain of lipid bilayer membranes. *Biophys. J.* **63:**78–88

Xiang, T.-X., Xu, Y.-H., Anderson, B.D. 1998. The barrier domain for solute permeation varies with lipid bilayer phase structure. *J. Membrane Biol.* **165:**77–90

Xiang, T.-X., Anderson, B.D. 1998. Influence of chain ordering on the selectivity of dipalmitoylphosphatidylcholine bilayer membranes for permeant size and shape. *Biophys. J.* **75:**2658–2671